Applied Mathematics and Nonlinear Sciences 2(2) (2017) 529–542

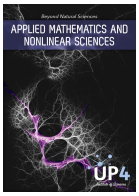

Applied Mathematics and Nonlinear Sciences

http://journals.up4sciences.org

# Investigation of the effect of albedo and oblateness on the circular restricted four variable bodies problem

Abdullah A. Ansari †

Department of Mathematics, College of Science Al-Zulfi, Majmaah University, 11932
Kingdom of Saudi Arabia

**Submission Info**

Communicated by Elbaz I. Abouelmagd
Received 9th February 2017
Accepted 12th December 2017
Available online 12th December 2017

## Abstract

The present paper investigates the motion of the variable infinitesimal body in circular restricted four variable bodies problem. We have constructed the equations of motion of the infinitesimal variable mass under the effect of source of radiation pressure due to which albedo effects are produced by another two primaries and one primary is considered as an oblate body which is placed at the triangular equilibrium point of the classical restricted three-body problem and also the variation of Jacobi Integral constant has been determined. We have studied numerically the equilibrium points, Poincaré surface of sections and basins of attraction in five cases (i. Third primary is placed at one of the triangular equilibrium points of the classical restricted three-body problem, ii. Variation of masses, iii. Solar radiation pressure, iv. Albedo effect, v. Oblateness effect.) by using Mathematica software. Finally, we have examined the stability of the equilibrium points and found that all the equilibrium points are unstable.

**Keywords:** Albedo, Oblate body, Triangular equilibrium points, Stationary Points, Poincaré surface of sections, Basins of Attraction.
**AMS 2010 codes:** 70F15, 85A20, 70F05.

## 1 Introduction

Few-body problem attract many scientists for a long time in celestial mechanics and dynamical astronomy. The restricted three-body problem and four-body problem with many perturbations like different shapes of the primaries, resonance, variable mass of the primaries as well as infinitesimal body, Coriolis and centrifugal forces, Pointing-Robertson drag, solar radiation pressure and albedo effects etc., have been studied by many scientists. Simó [36] investigated the linear stability of the relative Lagrangian solutions in the four-body problem. Hadjidemetriou [17]studied the periodic orbits of fourth body in the restricted four-body problem with respect to rotating frame. Michalodmitrakis [27] generalized the restricted three-body problem to the restricted four-body

†Corresponding author.
Email address: a.ansari@mu.edu.sa

ISSN 2444-8656 doi:10.21042/AMNS.2017.2.00044

problem and studied about the equilibrium points, regions of possible motion and periodic orbits. Kalvouridis et al. in the series of three papers [20,21] and [22] investigated the equilibrium points and stability in the restricted four-body problem under the effect of oblateness and radiation pressure. And also performed the zero-velocity surface and curves. Baltagiannis et al. [14] shown that equilibrium points depend on the mass of the primaries in the restricted four-body problem. Papadauris et al. [31,32] investigated the existence, locations, stability and periodic orbits of the equilibrium points in and out of the orbital plane in the photo-gravitational circular restricted four-body problem. Ansari [1] studied the periodic orbits in the restricted four-body problem around lagrangian points in three cases. In the first case, he has considered all three primaries as spherical in shape. In the second case, he has taken one of the three primaries as an oblate body. And in the third and last case, he has taken two of the primaries as oblate body and all the three primaries are source of radiation pressure. Falaye [16] investigated the stability of the equilibrium points in the restricted four-body problem under the effects of oblateness and solar radiation pressure and found that these equilibrium points are unstable. Arribas et al. [22] investigated the equilibria of the symmetric collinear restricted four-body problem where primaries are placed in a collinear central configuration with both masses and radiation pressure of the peripheral bodies are equal. Papadakis [30] performed the 21 families of simple 3D symmetric periodic orbits as well as the typical orbits of all symmetry type 3D orbits in the circular restricted four-body problem. After examined the stability, he illustrated the characteristic curves and stability diagrams of families of 3D periodic orbits. Asique et al. [10]– [13] studied the restricted four-body problem with different shapes of the primaries with solar radiation pressure. They have placed one of the primaries at the lagrangian points of the classical restricted three-body problem. They have illustrated the equilibrium points and zero-velocity curves for these models. Singh et al. [45,46] investigated in and out of plane equilibrium points in the circular restricted four-body problem with the effect of solar radiation pressure.

On the other-hand many scientists have studied about the albedo on these models. Anselmo et al. [8] performed the periodic perturbations of the satellite is the radiation pressure due to the sun-light reflected by the Earth. Rocco [34] evaluated the terrestrial albedo by using earth albedo model and orbital dynamics model and also calculated the irradiance at the satellite with radiant flux from each cells. Idrisi [18] investigated the existence and stability of the circular restricted three-body problem under the effect of albedo when smaller primary is an ellipsoid. Many scientists have investigated on these models with variable masses as Jeans [19], Meshcherskii [26], Shrivastava et al. [35], Lichtenegger [24], Singh et al. [37]- [41], Lukyanov [25], Zhang et al. [44], Abouelmagd and Mostafa [2], Mittal et al. [28], Ansari [3]- [6], etc. And also many scientists have explained the basins of attraction in these models as Douskos [15], Kumari and Kushvah [23], Paricio [33], Ansari [5,6], Zotos [45]- [48], etc.

This paper deals the motion of the infinitesimal body in the circular restricted four-body problem in which the masses of the primaries as well as the mass of the infinitesimal body vary and also one of the primaries is taken as source of radiation pressure due to which albedo effects are produced and another primary is considered as oblate body. We have studied this problem in various sections. In the statement of the problem and equations of motion section, we have constructed the equations of motion of the infinitesimal variable mass under the effect of these perturbations where the third primary is fixed at the triangular equilibrium point of the classical restricted three-body problem and also the variation of Jacobi Integral constant has been determined. In the computational work section, we have plotted numerically the equilibrium points, Poincaré surface of sections and basins of attraction in five cases by using Mathematica software. In the stability section, we have examined the stability of the equilibrium points under the effect of the perturbations. Finally, we have concluded the problem.

## 2 Statement of the problem and equations of motion

Let $m_1(t), m_2(t), m_3(t)$ and $m(t)$ be four variable masses ($m_1(t) > m_2(t) >> m_3(t)$). The configuration of the $m_1(t), m_2(t)$ and $m(t)$ is taken as the restricted three-body problem. The third primary $m_3(t)$ is considered as

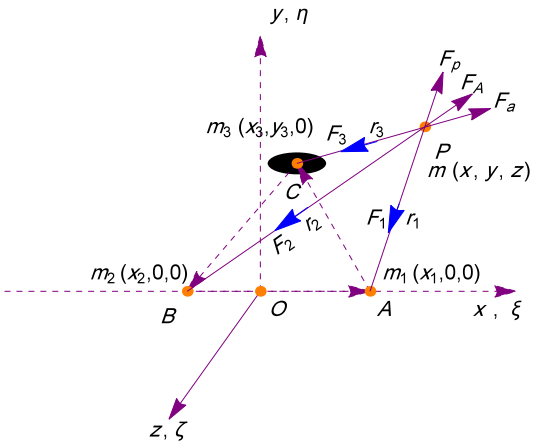


**Fig. 1** Configuration of the problem in CRFVBP with the effect of oblateness and Albedo.

so small that it is not influencing the motion of the primaries $m_1(t)$ and $m_2(t)$. Thus the center of the rotation of the system remains the same as for the bodies $m_1(t)$ and $m_2(t)$. The body $m_3(t)$ is placed at one of the triangular equilibrium points of the R3BP. $m(t)$ is moving in the space under the influence of these three primaries but not influencing them. In this way these four variable bodies formed the restricted circular four-body problem.
Here we have considered $m_3(t)$ as oblate body with oblateness factor $\sigma$ (the shape of the oblate body remain same though the mass is variable) and $m_1(t)$ is a source of radiations($F_p$)due to these radiations, $m_2(t)$ and $m_3(t)$ produce albedo $F_A$ and $F_a$ respectively (i.e. Albedo = (radiation reflected back into the space)/(incident radiation)). The infinitesimal body $m(t)$ is moving in the space under the gravitational forces $F_1, F_2$ and $F_3$ of the primaries respectively. The total force on infinitesimal body will be $F = F_1(1-p_1)+F_2(1-p_2)+F_3(1-p_3)$. Where $0 \leq p_1 = F_p/F_1 < 1, 0 \leq p_2 = F_A/F_2 < p_1, 0 \leq p_3 = F_a/F_3 < p_1$. The line joining $m_1(t)$ and $m_2(t)$ is taken as x-axis and are moving around their common center of mass which is taken as origin $O$ and the line perpendicular to the x-axis and passing through the origin is considered as y-axis, the line passing through the origin and perpendicular to the plane of motion of the primaries is taken as z-axis. Let us consider the synodic coordinate system, initially coincide with the inertial coordinate system, and revolving with angular velocity $\omega(t)$ about z-axis. Let the coordinates of $m_1(t)$, $m_2(t)$, $m_3(t)$ and $m(t)$ in the rotating frame be $(x_1,0,0),(x_2,0,0),(x_3,y_3,0)$ and $(x,y,z)$ respectively (Fig. 1). Following the procedure given in Ansari [7], we can write the equations of motion of the infinitesimal variable mass in the rotating coordinate system when the variation of mass is non-isotropic with zero momentum as

$$\begin{cases} \frac{\dot{m}(t)}{m(t)}(\dot{x}-\omega(t)\,y)+(\ddot{x}-\dot{\omega}(t)\,y-2\omega(t)\,\dot{y}-\omega^2(t)x) \\ =-\frac{\mu_1(t)(x-x_1)(1-p_1)}{r_1^3}-\frac{\mu_2(t)(x-x_2)(1-p_2)}{r_2^3}-\frac{\mu_3(t)(x-x_3)(1-p_3)}{r_3^3} \\ \qquad -\frac{3\mu_3(t)(x-x_3)(1-p_3)\sigma}{2r_3^5}, \\ \frac{\dot{m}(t)}{m(t)}(\dot{y}+\omega(t)\,x)+(\ddot{y}+\dot{\omega}(t)\,x+2\omega(t)\,\dot{x}-\omega^2(t)\,y) \\ \quad =-\frac{\mu_1(t)y(1-p_1)}{r_1^3}-\frac{\mu_2(t)y(1-p_2)}{r_2^3}-\frac{\mu_3(t)y(1-p_3)}{r_3^3} \\ \qquad -\frac{3\mu_3(t)(y-y_3)(1-p_3)\sigma}{2r_3^5}, \\ \frac{\dot{m}(t)}{m(t)}\dot{z}+\ddot{z}=-\frac{\mu_1(t)z(1-p_1)}{r_1^3}-\frac{\mu_2(t)z(1-p_2)}{r_2^3}-\frac{\mu_3(t)z(1-p_3)}{r_3^3} \\ \qquad -\frac{3\mu_3(t)z(1-p_3)\sigma}{2r_3^5}. \end{cases} \tag{1}$$

where, $r_i^2=(x-x_i)^2+(y-y_i)^2+z^2$ are the distances from the primaries to the infinitesimal body in the rotating coordinate system respectively, $\mu_i(t)=G\,m_i(t),(i=1,2,3)$.
Using Meshcherskii transformation
$x=\xi R(t),\ y=\eta R(t),\ z=\zeta R(t),\frac{dt}{d\tau}=R^2(t),r_i=\rho_i R(t),\omega(t)=\frac{\omega_0}{R^2(t)},x_i=\xi_i R(t),y_i=\eta_i R(t),\mu(t)=\mu_1(t)+\mu_2(t)=\frac{\mu_0}{R(t)},\mu_i(t)=\frac{\mu_{i0}}{R(t)},m(t)=\frac{m_0}{R(t)},R(t)=\sqrt{\alpha t^2+2\beta t+\gamma}$,
where $\alpha,\beta,\gamma,\mu_0,\mu_{i0},m_0$ are constants for $i=1,2,3$.
The system (1) becomes

$$\begin{cases} \xi''-2\omega_0\eta'-(\alpha t+\beta)\xi'=\frac{\partial W}{\partial \xi}, \\ \eta''+2\omega_0\xi'-(\alpha t+\beta)\eta'=\frac{\partial W}{\partial \eta}, \\ \zeta''-(\alpha t+\beta)\zeta'=\frac{\partial W}{\partial \zeta}. \end{cases} \tag{2}$$

where,

$$W=\tfrac{1}{2}((\alpha t+\beta)^2+\omega_0^2-(\alpha\gamma-\beta^2))(\xi^2+\eta^2)+\tfrac{1}{2}((\alpha t+\beta)^2-(\alpha\gamma-\beta^2))\zeta^2-(\alpha t+\beta)\xi\eta$$
$$+\frac{\mu_{10}(1-p_1)}{\rho_1}+\frac{\mu_{20}(1-p_2)}{\rho_2}+\frac{\mu_{30}(1-p_3)}{\rho_3}+\frac{\mu_{30}(1-p_3)\sigma}{2\rho_3^3},$$
$$\rho_i^2=(\xi-\xi_i)^2+(\eta-\eta_i)^2+\zeta^2.$$

Prime ($'$) is the differentiation w.r.to $\tau$. Taking unit of mass, distance and time at initial time $t_0$ such that

$$\mu_0=1,\ \xi_1+\xi_2=1,\ G=1,\ \omega_0=1,\ \alpha t_0+\beta=\alpha_1(constant).$$

Introducing the new mass parameter as $\mu_{10}=1-\upsilon,\mu_{20}=\upsilon,\mu_{30}=\alpha_2\upsilon$, where $\alpha_2<<1$ and $\upsilon$ is the ratio of the mass of the primary $m_2$ to the total mass of the primaries $m_1$ and $m_2$.
Finally, the system (2) becomes

$$\begin{cases} \xi''-2\eta'-\alpha_1\xi'=\frac{\partial U}{\partial \xi}, \\ \eta''+2\xi'-\alpha_1\eta'=\frac{\partial U}{\partial \eta}, \\ \zeta''-\alpha_1\zeta'=\frac{\partial U}{\partial \zeta}. \end{cases} \tag{3}$$

where, $U = \frac{1}{2}(\alpha_1^2+k)(\xi^2+\eta^2+\zeta^2) - \frac{1}{2}\zeta^2 - \alpha_1\xi\eta + \frac{(1-\upsilon)(1-p_1)}{\rho_1} + \frac{\upsilon(1-p_2)}{\rho_2} + \frac{\alpha_2\upsilon(1-p_3)}{\rho_3} + \frac{\alpha_2\upsilon(1-p_3)\sigma}{2\rho_3^3}$,

$\rho_i^2 = (\xi-\xi_i)^2 + (\eta-\eta_i)^2 + \zeta^2, \alpha\gamma - \beta^2 = 1-k$ and $(\xi_1,\eta_1) = (\upsilon,0)$,$(\xi_2,\eta_2) = (1-\upsilon,0)$, $(\xi_3,\eta_3) = (\upsilon - \frac{1}{2}, \frac{\sqrt{3}}{2})$.

If there are constant masses then there is a constant motion (i.e Moulton [29]), the Jacobi Integral Constant defined as

$$J_{IC} = 2U - 2((\xi')^2 + (\eta')^2 + (\zeta')^2), \tag{4}$$

Multiplying in the first equation of (3) by $\xi'$, in the second equation of (3) by $\eta'$ and in the third equation of (3) by $\zeta'$ and add and using equation (4), we get the variation of the Jacobi Integral Constant as

$$\frac{dJ_{IC}}{d\tau} = -2\alpha_1((\xi')^2 + (\eta')^2 + (\zeta')^2), \tag{5}$$

Where $J_{IC}$ is the Jacobi Integral Constant.

## 3 Computational work

In this section, we have drawn the locations of equilibrium points, the Poincaré surfaces of section and the basins of attraction for five different cases by using Mathematica software (in all the calculations $\upsilon = 0.019, \alpha_2 = 0.01$):

a. Third primary is placed at one of the Lagrangian points of the classical restricted three-body problem
(i.e. $k = 1, \alpha_1 = 0, p_1 = 0, p_2 = 0, p_3 = 0, \sigma = 0$),
b. Variation of masses
(i.e. $k = 0.4, \alpha_1 = 0.2, p_1 = 0, p_2 = 0, p_3 = 0, \sigma = 0$),
c. Solar radiation pressure
(i.e. $k = 0.4, \alpha_1 = 0.2, p_1 = 0.5, p_2 = 0, p_3 = 0, \sigma = 0$),
d. Albedo effect
(i.e. $k = 0.4, \alpha_1 = 0.2, p_1 = 0.5, p_2 = 0.3, p_3 = 0.2, \sigma = 0$),
e. Oblateness effect
(i.e. $k = 0.4, \alpha_1 = 0.2, p_1 = 0.5, p_2 = 0.3, p_3 = 0.2, \sigma = 0.01$).

### 3.1 Equilibrium points during in-plane and out of plane motions

The solutions of $U_\xi = 0$, $U_\eta = 0$, and $U_\zeta = 0$, will be the location of equilibrium points but the solutions of these equations represent the location of equilibrium points during in-plane motions when $(\xi \neq 0, \eta \neq 0, \zeta = 0), (Fig.2)$ and represent the location of equilibrium points of the out of plane when $(\xi \neq 0, \eta = 0, \zeta \neq 0), (Fig.3)$ and $(\xi = 0, \eta \neq 0, \zeta \neq 0), (Fig.4)$. At the equilibrium points, all the derivatives of the co-ordinates with respect to the time will be zero. Therefore the infinitesimal body will stay at these points with zero velocity. Hence the singularities are known as stationary points. Where

$$U_\xi = (\alpha_1^2+k)\xi - \alpha_1\eta - \frac{(1-\upsilon)(\xi-\xi_1)(1-p_1)}{\rho_1^3} - \frac{\upsilon(\xi-\xi_2)(1-p_2)}{\rho_2^3} - \frac{\upsilon_3(\xi-\xi_3)(1-p_3)}{\rho_3^3} - \frac{3\alpha_2\upsilon(\xi-\xi_3)(1-p_3)\sigma}{2\rho_3^5}, \tag{6}$$

$$U_\eta = (\alpha_1^2+k)\eta - \alpha_1\xi - \frac{(1-p_1)(1-\upsilon)\eta}{\rho_1^3} - \frac{(1-p_2)\upsilon\eta}{\rho_2^3} - \frac{\upsilon_3(\eta-\eta_3)(1-p_3)}{\rho_3^3} - \frac{3\alpha_2\upsilon\eta(1-p_3)\sigma}{2\rho_3^5}, \tag{7}$$

$$U_\zeta = (\alpha_1^2+k-1)\zeta - \frac{(1-p_1)(1-\upsilon)\zeta}{\rho_1^3} - \frac{(1-p_2)\upsilon\zeta}{\rho_2^3} - \frac{\upsilon_3\zeta(1-p_3)}{\rho_3^3} - \frac{3\alpha_2\upsilon\zeta(1-p_3)\sigma}{2\rho_3^5}. \tag{8}$$

#### 3.1.1 During in-plane motion (i.e. $\xi \neq 0, \eta \neq 0, \zeta = 0$) locations of lagrangian points

During in-plane motion, we have plotted graphs for the locations of the lagrangian points in five cases. We found six lagrangian points in which three points $(L_1, L_2, L_3)$ are collinear and rest three points $(L_4, L_5, L_6)$ are non-collinear when third primary is placed at one of the lagrangian points of the classical restricted circular three-body problem (Fig. $2(a)$ points with blue color). It is observed that the lagrangian points $(L_1, L_4, L_5, L_6)$ and $(L_2, L_3)$ lie left side and right side of the origin respectively. In the variable mass case, we found six lagrangian points (Fig. $2(b)$ points with green color) in which points $(L_2, L_3, L_6)$ and $(L_1, L_4, L_5)$ lie left side and right side of the origin respectively. Here $(L_3, L_4)$ and $(L_5, L_6)$ are symmetrical and rest points are non-symmetrical. In the rest three cases, we found eight lagrangian points with slight different locations (Fig. $2(c)$ points with red color, Fig. $2(d)$ points with black color, Fig. $2(e)$ points with magenta color). In all the figures black stars denote the locations of the primaries respectively.

#### 3.1.2 During out of plane (i.e. $\xi \neq 0, \eta = 0, \zeta \neq 0$ and $\xi = 0, \eta \neq 0, \zeta \neq 0$)the locations of lagrangian points

During out of plane (i.e. $\xi \neq 0, \eta = 0, \zeta \neq 0$), we found three lagrangian points on the $\xi$-axis in all the five cases (Fig. $3(a)$ points in blue color, Fig. $3(b)$ points in green color, Fig. $3(c)$ points with red color, Fig. $3(d)$ points with black color, Fig. $3(e)$ points with magenta color). In all the cases, the points $L_1$ and $(L_2, L_3)$ lie left and right side of the origin with slight different locations respectively. The black stars denote the locations of the primaries $m_1$ and $m_2$.
On the other hand, during the out of plane (i.e. $\xi = 0, \eta \neq 0, \zeta \neq 0$ ), we found three lagrangian points $(Fig.4)$ in all five cases. The points $L_1$ and $L_3$ lie left and right side of the origin respectively but the point $L_2$ lies at the origin. It is also observed from the Figure 4 that lagrangian points are moving away from the origin from the first case to the variable mass case and then toward the origin in the other cases.

### 3.2 Poincaré Surface of Section

We also have drawn the Poincaré surface of sections for five cases in both the $(\xi - \xi')-$plane (Fig.5 (i)) and the $(\eta - \eta')-$plane (Fig.5 (ii), Fig. 5 (iii)). It is observed that in the $\xi - \xi'$-plane, the surfaces are shrinking and in the $\eta - \eta'$-plane, the surfaces first expanding and then shrinking.

### 3.3 Basins of attraction

In this section, we have drawn the basins of attraction for the circular restricted four variable bodies problem in which we have taken one primary as solar radiation pressure due to which other two primaries produced albedo and also one of the primaries as an oblate body, by using Newton-Raphson iterative method for the five cases (i. Third primary is placed at one of the lagrangian points of the restricted three-body problem, ii. Variation of mass case, iii. Solar radiation pressure effect, iv. Albedo effect, v. Oblateness effect). The algorithm of our problem is given by

$$\begin{cases} \xi_{n+1} = \xi_n - \left( \frac{U_\xi U_{\eta\eta} - U_\eta U_{\xi\eta}}{U_{\xi\xi} U_{\eta\eta} - U_{\xi\eta} U_{\eta\xi}} \right)_{(\xi_n, \eta_n)}, \\ \eta_{n+1} = \eta_n - \left( \frac{U_\eta U_{\xi\xi} - U_\xi U_{\eta\xi}}{U_{\xi\xi} U_{\eta\eta} - U_{\xi\eta} U_{\eta\xi}} \right)_{(\xi_n, \eta_n)}. \end{cases} \tag{9}$$

Where $\xi_n, \eta_n$ are the values of $\xi$ and $\eta$ coordinates of the $n^{th}$ step of the Newton-Raphson iterative process. If the initial point converges rapidly to one of the lagrangian points then this point $(\xi, \eta)$ is a member of the basin of attraction of the root. This process stops when the successive approximation converges to an attractor. We used color code for the classification of the lagrangian points on the $(\xi, \eta)-$plane. In the first case (Fig. 6), $L_1, L_2, L_3$ represent cyan color regions, $L_4, L_5, L_6$ represents light blue color regions. The basins of attraction corresponding to the lagrangian points $L_1, L_2, L_3, L_4, L_5, L_6$ extend to infinity. In the variable mass case (Fig. 7), $L_1$ represents cyan color region, $L_2, L_3, L_5$ represent light blue color regions, $L_4$ and $L_6$ represent light green color regions. The basins of attraction corresponding to the lagrangian point $L_1$ cover finite area but corresponding to the lagrangian

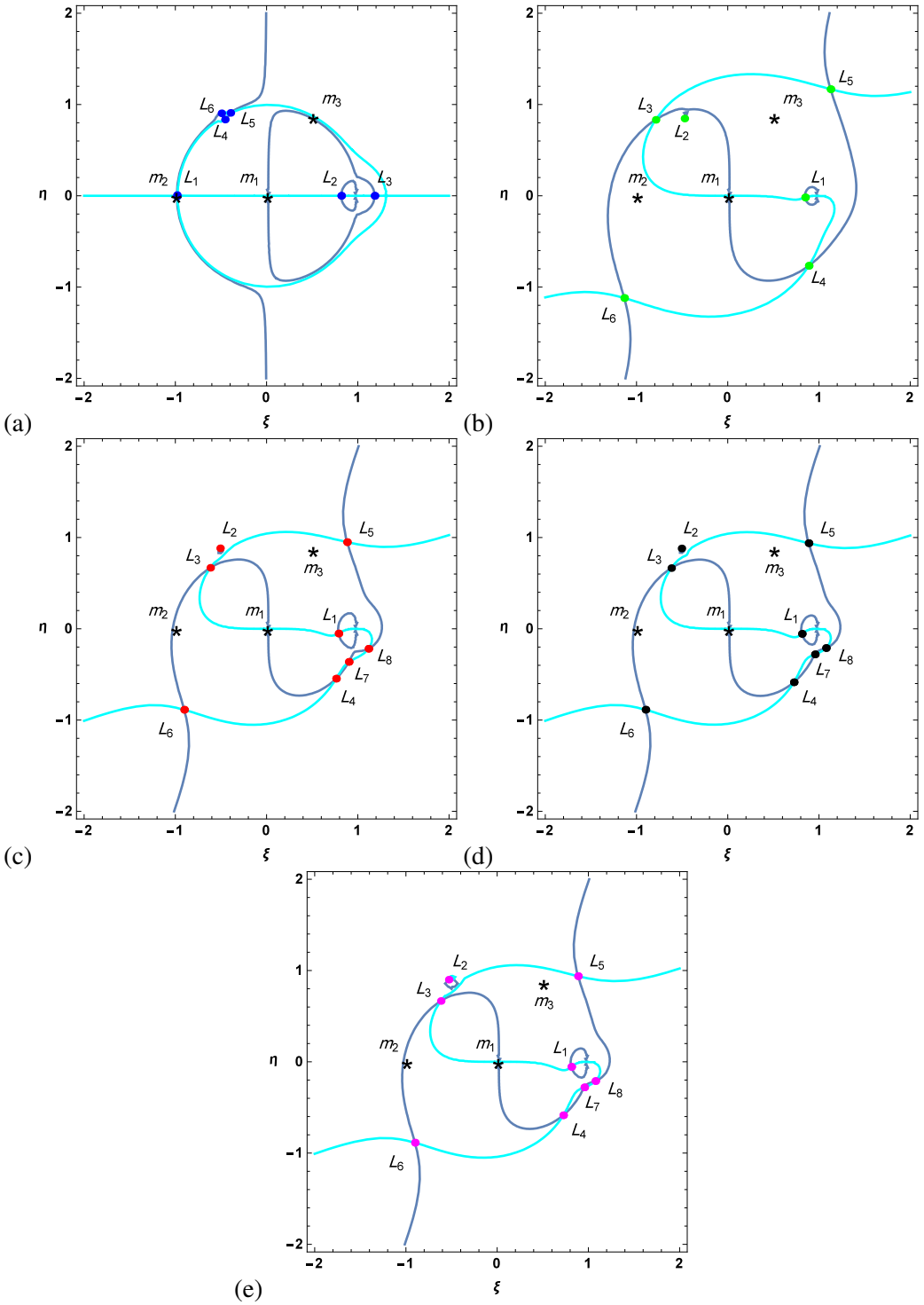


**Fig. 2** The locations of lagrangian points during in-plane motion (i.e. $\xi \neq 0, \eta \neq 0, \zeta = 0$) in five cases: (a). Third primary is placed at one of the lagrangian points of the classical circular restricted three-body problem (points with blue color), (b). Variation of masses (points with green color), (c). Solar radiation pressure (points with red color), (d). Albedo effect (points with black color), (e). Oblateness effect (points with magenta color).

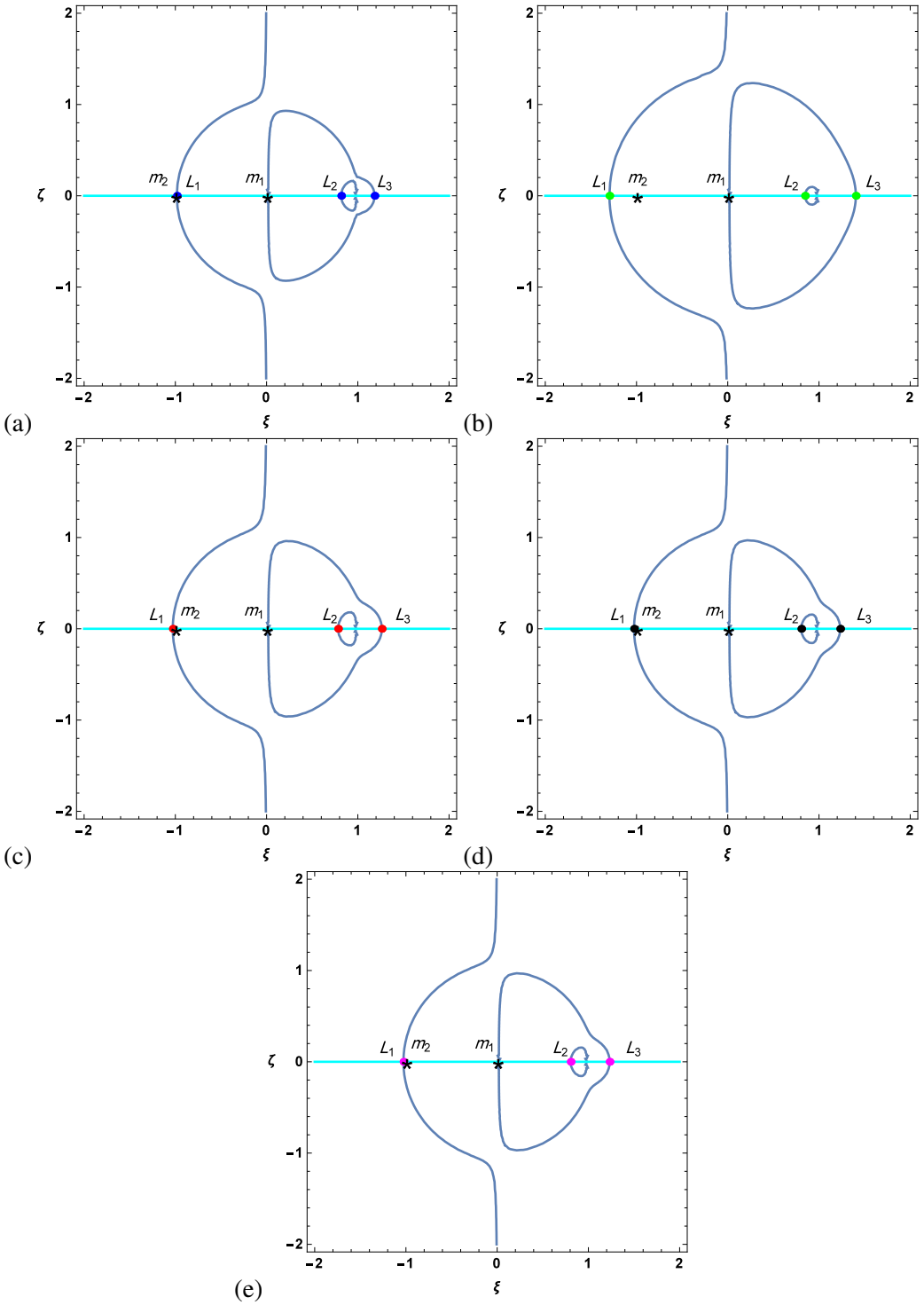


**Fig. 3** The locations of lagrangian points during out of plane motion (i.e. $\xi \neq 0, \eta = 0, \zeta \neq 0$ ) in five cases: (a). Third primary is placed at one of the lagrangian points of the classical circular restricted three-body problem (points with blue color), (b). Variation of masses (points with green color), (c). Solar radiation pressure (points with red color), (d). Albedo effect (points with black color), (e). Oblateness effect (points with magenta color).

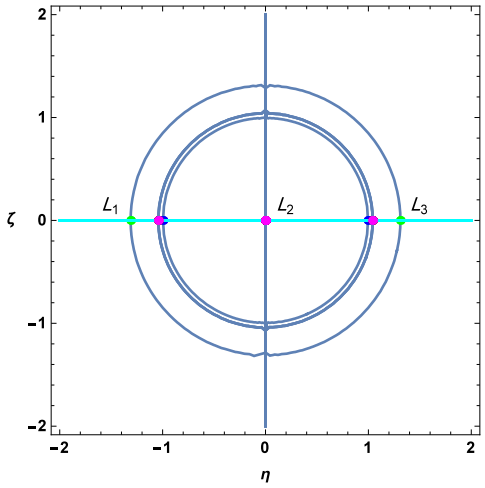


**Fig. 4** The locations of lagrangian points during out of plane motion (i.e.$\xi = 0, \eta \neq 0, \zeta \neq 0$) in five cases: (a). Third primary is placed at one of the lagrangian points of the classical circular restricted three-body problem (points with blue color), (b). Variation of masses (points with green color), (c). Solar radiation pressure (points with red color), (d). Albedo effect (points with black color), (e). Oblateness effect (points with magenta color).

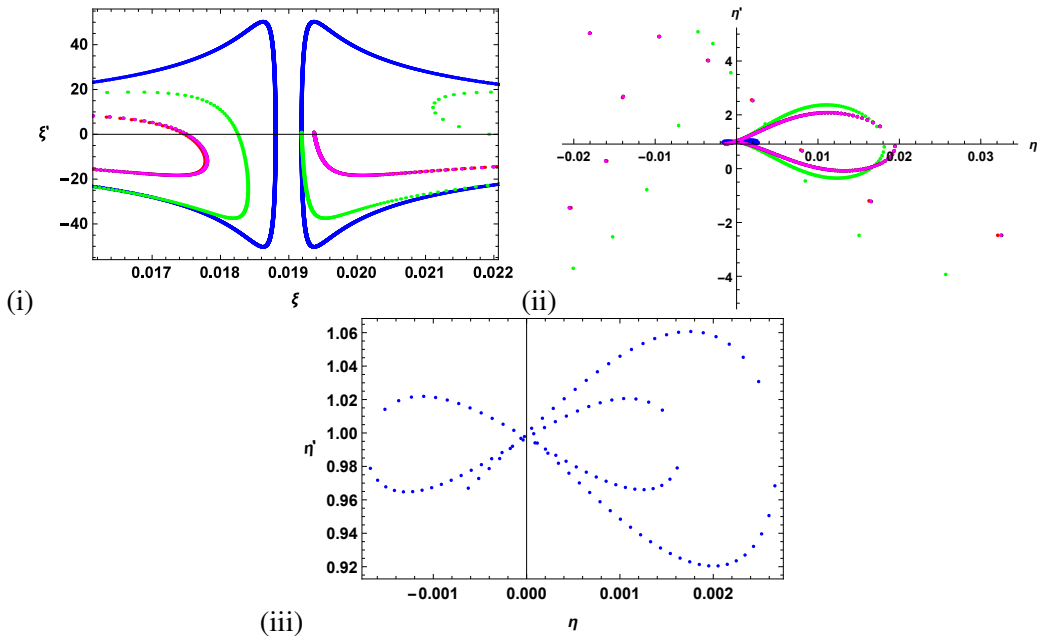


**Fig. 5** Poincaré surface of sections for five cases: (a). Third primary is placed at one of the lagrangian points of the classical circular restricted three-body problem (with blue color), (b). Variation of masses (with green color), (c). Solar radiation pressure (with red color), (d). Albedo effect (with black color), (e). Oblateness effect (with magenta color). (i) Poincaré surface of sections in $\xi - \xi'$-plane, (ii) Poincaré surface of sections in $\eta - \eta'$-plane, (iii) Zoomed part of figure (ii) near the origin.

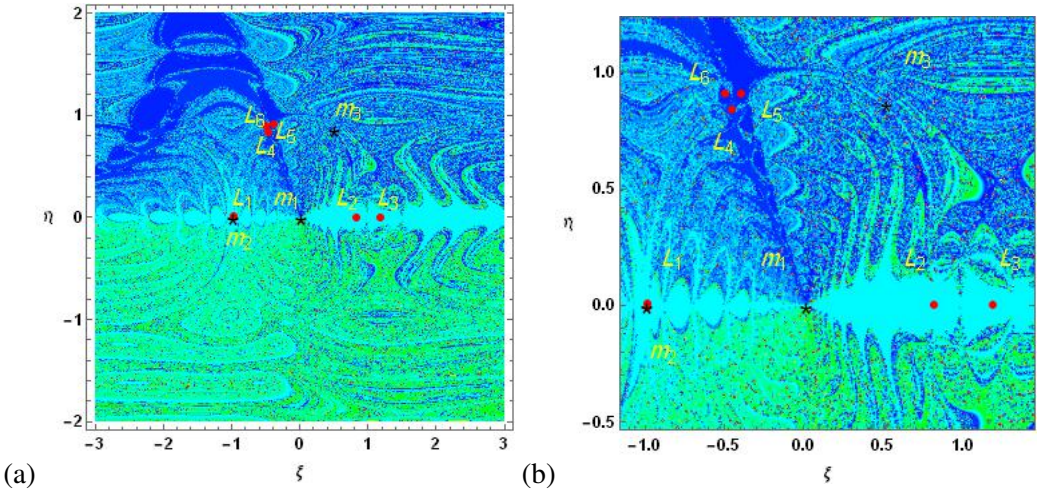


**Fig. 6** (a): The basin of attraction for the case when third primary is placed at one of the lagrangian points of the classical circular restricted three- body problem. (b): Zoomed image of (a) near the lagrangian configuration.

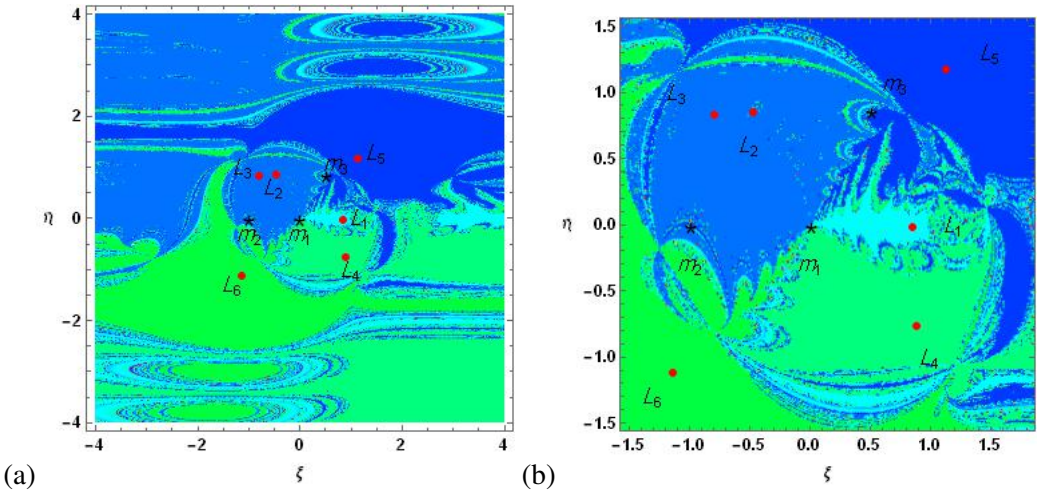


**Fig. 7** (a): The basin of attraction for the variable mass case. (b): Zoomed image of (a) near the lagrangian configuration.

points $L_2, L_3, L_4, L_5, L_6$ extend to infinity. While in the rest three cases (Fig. 8, Fig. 9, Fig. 10), $L_1$ represents cyan color region, $L_2$, $L_3$ represent light blue, $L_5$ represents blue color region and $L_4, L_6, L_7, L_8$ represent light green color regions. The basins of attraction corresponding to the all lagrangian points $L_2, L_3, L_4, L_5, L_6, L_7, L_8$ extend to infinity except $L_1$ which covers finite area. In this way a complete view of the basin structures created by the attractors. We can observe in detail from the zoomed part of all the figures in Fig. 6(b), Fig. 7(b), Fig. 8(b), Fig. 9(b), Fig. 10(b). The black points and black stars denote the location of the lagrangian points and the primaries respectively.

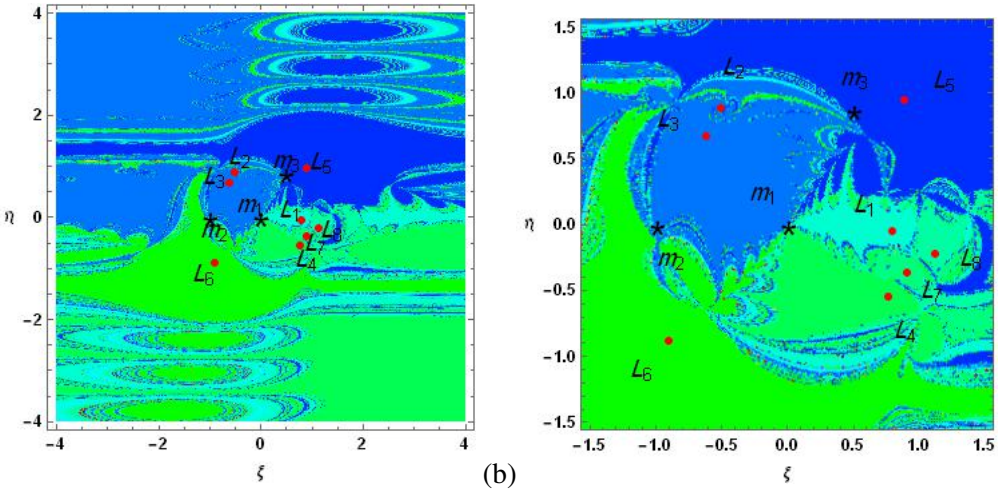


**Fig. 8** (a): The basin of attraction for the solar radiation pressure case. (b): Zoomed image of (a) near the lagrangian configuration.

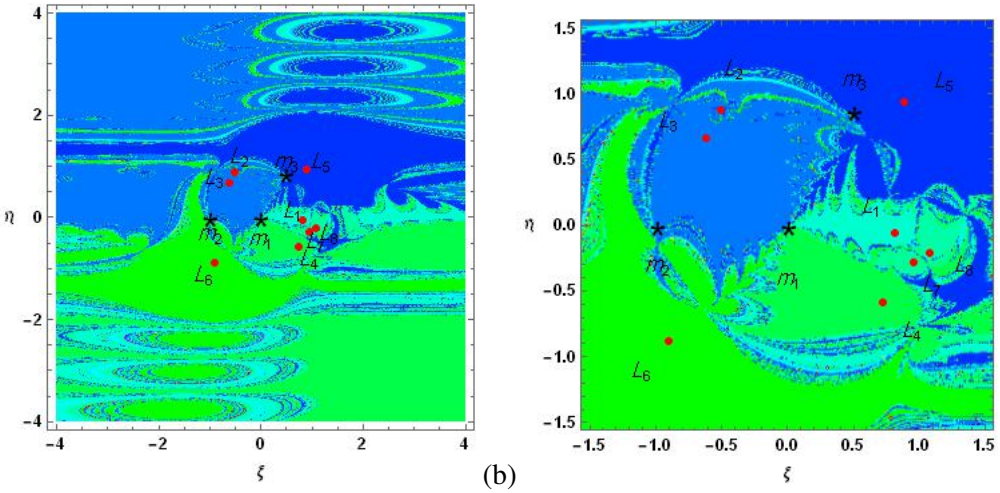


**Fig. 9** (a): The basin of attraction for the Albedo case. (b): Zoomed image of (a) near the lagrangian configuration.

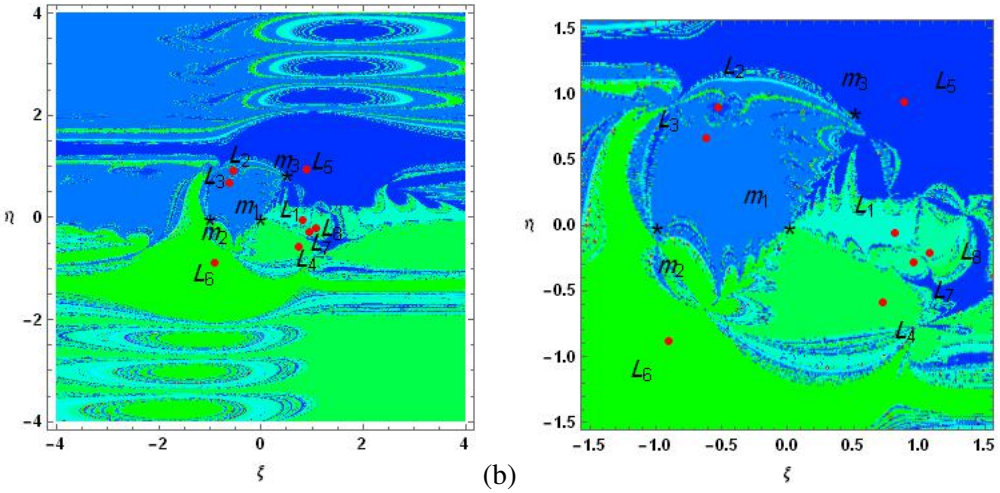


**Fig. 10** (a): The basin of attraction for the oblateness case. (b): Zoomed image of (a) near the lagrangian configuration.

## 4 Stability of the equilibrium points

We can examine the stability of the equilibrium points under the effect of Albedo and oblateness when all the masses are varying, by taking $\xi = \xi_0 + \xi_d,\ \eta = \eta_0 + \eta_d,\ \zeta = \zeta_0 + \zeta_d$ in system (3), we get

$$\begin{cases} \xi_d'' - 2\,\eta_d' - \alpha_1 \xi_d' = \xi_d\, U^0_{\xi\xi} + \eta_d\, U^0_{\xi\eta} + \zeta_d\, U^0_{\xi\zeta} \\ \eta_d'' + 2\,\xi_d' - \alpha_1 \eta_d' = \xi_d\, U^0_{\eta\xi} + \eta_d\, U^0_{\eta\eta} + \zeta_d\, U^0_{\eta\zeta} \\ \zeta_d'' - \alpha_1 \zeta_d' \quad\ = \xi_d\, U^0_{\zeta\xi} + \eta_d\, U^0_{\zeta\eta} + \zeta_d\, U^0_{\zeta\zeta} \end{cases} \tag{10}$$

Where $\xi_d,\ \eta_d$ and $\zeta_d$ are the small displacements of the infinitesimal body from the equilibrium point. The superscript zero denotes the value at the equilibrium point.

To solve system (10), let $\xi_d = C_1 e^{\lambda\tau},\ \eta_d = C_2 e^{\lambda\tau},\ \zeta_d = C_3 e^{\lambda\tau}$, where $C_1, C_2$ and $C_3$ are constant parameters. Substituting these values in system (10) and rearranging, we get:

$$\begin{cases} C_1(\lambda^2 - \alpha_1\lambda - U^0_{\xi\xi}) - C_2(2\lambda + U^0_{\xi\eta}) - C_3 U^0_{\xi\zeta} = 0, \\ C_1(2\lambda - U^0_{\eta\xi}) + C_2(\lambda^2 - \alpha_1\lambda - U^0_{\eta\eta}) - C_3 U^0_{\eta\zeta} = 0, \\ -C_1 U^0_{\zeta\xi} - C_2 U^0_{\zeta\eta} + C_3(\lambda^2 - \alpha_1\lambda - U^0_{\zeta\zeta}) = 0. \end{cases} \tag{11}$$

The system (11), will have a non-trivial solution for $C_1, C_2$ and $C_3$ if

$$\begin{vmatrix} \lambda^2 - \alpha_1\lambda - U^0_{\xi\xi} & -(2\lambda + U^0_{\xi\eta}) & -U^0_{\xi\zeta} \\ 2\,\lambda - U^0_{\eta\xi} & \lambda^2 - \alpha_1\lambda - U^0_{\eta\eta} & -U^0_{\eta\zeta} \\ -U^0_{\zeta\xi} & -U^0_{\zeta\eta} & \lambda^2 - \alpha_1\lambda - U^0_{\zeta\zeta} \end{vmatrix} = 0,$$

which is equivalent to

$$\begin{aligned} &\lambda^6 - 3\alpha_1\lambda^5 + \lambda^4(4 + 3\alpha_1^2 - U^0_{\xi\xi} - U^0_{\eta\eta} - U^0_{\zeta\zeta}) + \alpha_1\lambda^3(-4 - \alpha_1^2 + 2\,U^0_{\xi\xi} + 2\,U^0_{\eta\eta} + 2\,U^0_{\zeta\zeta}) \\ &+\lambda^2(-(U^0_{\xi\eta})^2 - (U^0_{\xi\zeta})^2 + U^0_{\xi\xi}\,U^0_{\eta\eta} - (U^0_{\eta\zeta})^2 - 4U^0_{\zeta\zeta} + U^0_{\xi\xi}U^0_{\zeta\zeta} + U^0_{\zeta\zeta}\,U^0_{\eta\eta} - \alpha_1^2\,U^0_{\xi\xi} - \alpha_1^2\,U^0_{\eta\eta} - \alpha_1^2\,U^0_{\zeta\zeta}) \\ &+\alpha_1\lambda((U^0_{\xi\eta})^2 + (U^0_{\xi\zeta})^2 - U^0_{\xi\xi}\,U^0_{\eta\eta} + (U^0_{\eta\zeta})^2 - U^0_{\xi\xi}\,U^0_{\zeta\zeta} - U^0_{\eta\eta}\,U^0_{\zeta\zeta}) \\ &+(U^0_{\xi\zeta})^2\,U^0_{\eta\eta} - 2\,U^0_{\xi\eta}\,U^0_{\xi\zeta}\,U^0_{\eta\zeta} + U^0_{\xi\xi}\,(U^0_{\eta\zeta})^2 + (U^0_{\xi\eta})^2\,U^0_{\zeta\zeta} - U^0_{\xi\xi}\,U^0_{\eta\eta}\,U^0_{\zeta\zeta} = 0, \end{aligned} \tag{12}$$

From the solution of the equation (12) we found that $\lambda$ has complex values in all the cases and at least one of them has positive real value. Hence all the equilibrium points are unstable.

## 5 Conclusions

In this paper, we have investigated the effect of Albedo and oblateness of the primary in the circular restricted four-body problem with variable masses. We have determined the equations of motion, when the masses of the primaries as well as the infinitesimal body vary, which are different from the classical case by the variation parameters $\alpha_1$, $k$, oblateness factor $\sigma$ and the radiations effect $p_1$, $p_2$, $p_3$. Further the expression for the variation of Jacobi integral constant have been evaluated which is also depending on the variation parameter $\alpha_1$. We have plotted equilibrium points, Poincaré surface of sections and basins of attraction in five cases (i. Case when third primary is placed at one of the lagrangian points of the classical circular restricted three-body problem, ii. Variation of mass, iii. Solar radiation pressure effect, iv. Albedo effect, v. Oblateness effect) by using Mathematica software. The equilibrium points during in-plane motion (Fig. 2), we found six equilibrium points in which three are collinear and three are non-collinear equilibrium points in the first case, in the variable mass

case, we got one is collinear and rest five are non-collinear, while in the cases solar radiation pressure, albedo and oblateness, we found eight equilibrium points. During out-of-plane motions (i.e. $\xi \neq 0, \eta = 0, \zeta \neq 0$)(Fig. 3)and (i.e. $\xi = 0, \eta \neq 0, \zeta \neq 0$)(Fig. 4), we found three equilibrium points in all cases. The poincaré surface of sections have been determined in two phase spaces ($\xi - \xi'$ Fig. 5 (i) and $\eta - \eta'$ Fig. 5 (ii) ). In $\xi - \xi'$-plane, the poincaré surface of sections are shrinking and $\eta - \eta'$-plane, the poincaré surface of sections are first expanding and then shrinking . The Newton-Raphson basins of attraction have been studied in all five cases (Fig. 6, Fig. 7, Fig. 8, Fig. 9, Fig. 10). We used color code for the classification of the equilibrium points on the $(\xi - \eta)-$plane. These points will be clearly visible in the zoomed part of all the figures near the lagrangian configuration (ie. Fig. 6 b, Fig. 7 b, Fig. 8 b, Fig. 9 b, Fig. 10 b). Finally, we have examined the stability of the equilibrium points in the circular restricted four variable bodies problem with oblateness and albedo effect and found that all the equilibrium points are unstable.

## 6 Acknowledgement

We are thankful to the Deanship of Scientific Research and the Department of Mathematics, College of Science Al-Zulfi, Majmaah University, Kingdom of Saudi Arabia for providing all the research facilities. We are also grateful to the referee for his valuable suggestions.

## References

[1] Ansari, A. A, (2014),*Periodic orbits around lagrangian points of the circular restricted four-body problem. Invertis Journal of Science and Technology*. 7(1), 29-38.
[2] Abouelmagd, E. I., Mostafa, A.,(2015), *Out of plane equilibrium points locations and the forbidden movement regions in the restricted three-body problem with variable mass. Astrophys. Space Sci.* 357, 58, doi 10.1007/s10509-015-2294-7
[3] Ansari, A. A., (2016(a)), *Stability of the equilibrium points in the photogravitational circular restricted four body problem with the effect of perturbations and variable mass.Science International (Lahore)*. 28, 859- 866.
[4] Ansari, A. A., (2016(b)), *Stability of the equilibrium points in the circular restricted four body problem with oblate primary and variable mass. International Journal of Advanced Astronomy*. 4(1), 14-19. doi 10.14419/ijaa.v4i1.5831
[5] Ansari, A. A.(2016 (c)), *The Photogravitational Circular Restricted Four-body Problem with Variable Masses. Journal of Engineering and Applied Sciences*. 3(2), 30-38.
[6] Ansari, A. A.,(2017(a)), *The circular restricted four body problem with variable masses. Nonlinear Sci. Lett. A*. 8(3), 303-312.
[7] Ansari, A. A.,(2017(b)), *Effect of Albedo on the motion of the infinitesimal body in circular restricted three-body problem with variable masses. Italian J. of Pure and Applied Mathematics*. 38, 581-600.
[8] Anselmo, L., Farinella, P., Milani, A., Nobili, A. M.,(1983), *Effects of the earth-reflected sunlight on the orbit of the LAGEOS Satellite. Astron. Astrophys.*. 117, 3-8.
[9] Arribas, M., Abad, A., Elipe, A., Palacios, M.,(2016), *Out-of-plane equilibria in the symmetric collinear restricted four-body problem with radiation pressure.Astrophys. Space Sci.* 361, 270(8). 10.1007/s10509-016-2858-1
[10] Asique, M. C., et al.,(2015(a)),*On the R4BP when third primary is an oblate spheroid. Astrophys. Space Sci.* 357, 82(1). doi 10.1007/s10509-015-2235-5 13
[11] Asique, M. C., et al.,(2015(b)),*On the photogravitational R4BP when the third primary is an oblate/prolate spheroid. Astrophys. Space Sci.* 360, 13(1), doi 10.1007/s10509-015-2522-1 14
[12] Asique, M. C., et al., (2016), *On the photogravitational R4BP when the third primary is a triaxial rigid body. Astrophys. Space Sci.* 361, 379. doi 10.1007/s10509-016-2959-x
[13] Asique, M. C., et al.,(2017), *On the R4BP when Third Primary is an Ellipsoid. Journal of Astronaut. Sci.* 64, 231-250, doi 10.1007/s40295-016-0104-2
[14] Baltagiannis, A., Papadakis, K. E.,(2011), *Equilibrium points and their stability in the restricted four body problem. International Journal of Bifurcation and Chaos*. 21(8), 2179-2193, doi 10.1142/S0218127411029707
[15] Douskos, C. N.,(2010), *Collinear equilibrium points of Hill's problem with radiation pressure and oblateness and their fractal basins of attraction. Astrophys. Space Sci.* 326, 263-271. doi 10.1007/s10509-009-0213-5
[16] Falaye, B. J.,(2015), *Effect of Oblateness, Radiation and a Circular Cluster of Material Points on the Stability of Equilibrium Points in the Restricted Four-Body Problem. Few body system*. 56, 29-40, doi 10.1007/s00601-014-0922-3
[17] Hadjidemetriou, J. D.,(1980), *The Restricted Planetary 4-Body Problem.Celest. Mech.*. 21, 63-71.

[18] Idrisi, M. J.(2017), *A study of Libration Points in Modified CR3BP under Albedo Effect when smaller Primary is an Ellipsoid. J. of Astronaut. Sci.*, doi 10.1007/s40295-017-0115-7
[19] Jeans, J. H., (1928), *Astronomy and Cosmogony*, Cambridge University Press, Cambridge.
[20] Kalvouridis, T. J., Mavraganis, A. G.,(1995), *Equilibria and stability of the restricted photogravitational problem of 2 + 2 bodies*. *Astrophys. Space Sci.* 226(1), 137-148. doi 10.1007/BF00626906
[21] Kalvouridis, T. J.,(1996),*The oblate spheroids version of the restricted photogravitational 2+2 body problem. Astrophys. Space Sci.* 246(2), 219-227. doi 10.1007/BF00645642
[22] Kalvouridis, T. J., Arribas, M., Elipe, A.,(2006),*Dynamical properties of the restricted four-body problem with radiation pressure*. *Mechanics Research Communications*. 33, 811-817. doi 10.1016/j.mechrescom.2006.01.008
[23] Kumari, R., Kushvah, B. S.,(2014), *Stability regions of equilibrium points in the restricted four body problem with oblateness effects*. *Astrophys. Space Sci.* 349, 693-704. doi 10.1007/s10509-013-1689-6
[24] Lichtenegger, H.,(1984),*The dynamics of bodies with variable masses*. *Celest. Mech.* 34, 357-368.
[25] Lukyanov, L. G.,(2009), *On the restricted circular conservative three-body problem with variable masses*. *Astronomy Letters*. 35(5), 349-359.
[26] Meshcherskii, I. V.,(1952), *Works on the Mechanics of Bodies of Variable Mass*, GITTL, Moscow.
[27] Michalodmitrakis, M.,(1981), *The circular restricted four-body problem. Astrophys. Space Sci.* 75, 289-310.
[28] Mittal, A., et. al.,(2016), *Stability of libration points in the restricted four-body problem with variable mass. Astrophys. Space sci.* 361, 329, doi 10.1007/s10509-016-2901-2
[29] Moulton, F. R., (1914), *An introduction to celestial mechanic*, Second ed. Dover, New York.
[30] Papadakis, K. E.,(2016), *Families of three-dimensional periodic solutions in the circular restricted four-body Problem*. *Astrophys. Space Sci.* 361, 129. doi 10.1007/s10509-016-2713-4
[31] Papadouris, J. P., Papadakis, K. E.,(2013), *Equilibrium points in the photogravitational restricted four-body Problem*. *Astrophys. Space Sci.* 344, 21-38. doi 10.1007/s10509-012-1319-8
[32] Papadouris, J. P., Papadakis, K. E.,(2014), *Periodic solutions in the photogravitational restricted four-body problem*. *MNRAS*. 442, 1628-1639.
[33] Paricio, L. J. H.,(2016), *Bivariate Newton-Raphson method and toroidal attraction basins*. *Numerical Algo.* 71, 349-381. doi 10.1007/s11075-015-9996-3
[34] Rocco, E. M.,(2009), *Evaluation of the terestrial Albedo-Applied to some scientific missions*. *Space Sci. Rev.* 151, 135-147, doi 10.1007/s11214-009-9622-6
[35] Shrivastava, A. K., Ishwar, B.,(1983),*Equations of motion of the restricted problem of three bodies with variable mass*. *Celest. Mech.* 30, 323-328.
[36] Simo, C.,(1978), *Relative equilibrium solutions in the four body problem*. *Celest. Mech.* 18, 165-184.
[37] Singh, J., Ishwar, B.,(1984), *Effect of perturbations on the location of equilibrium points in the restricted problem of three bodies with variable mass*. *Celest. Mech.* 32, 297-305.
[38] Singh, J., Ishwar, B.,(1985), *Effect of perturbations on the stability of triangular points in the restricted problem of three bodies with variable mass*. *Celest. Mech.* 35, 201-207.
[39] Singh, J.,(2003),*Photogravitational restricted three body problems with variable mass*. *Indian Journal of Pure and Applied Math.* 32 (2), 335-341.
[40] Singh, J., Leke, O.,(2010), *Stability of photogravitational restricted three body problem with variable mass*. *Astrophys. Space Sci.* 326 (2), 305-314. doi 10.1007/s10509-009-0253-x
[41] Singh, J., Leke, O.,(2013), *Existence and Stability of Equilibrium Points in the Robe's Restricted Three-Body Problem with Variable Masses*. *International Journal of Astronomy and Astrophysics*. 3, 113-122. doi 10.4236/ijaa.2013.32013
[42] Singh, J.,Vincent, A. E.,(2016(a)),*Equilibrium points in the restricted four-body problem with radiation pressure*. *Few-Body Syst.* 57, 83-91. doi 10.1007/s00601-015-1030-8
[43] Singh, J.,Vincent, A. E.,(2016(b)),*Out-of-plane equilibrium points in the photogravitational restricted four-Body problem with oblateness*. *British Journal of Mathematics and Computer Science*. 19(5), 1-15. doi 10.9734/BJMCS/2016/29698
[44] Zhang, M. J., Zhao, C. Y., Xiong, Y. Q.,(2012), *On the triangular libration points in photo-gravitational restricted three body problem with variable mass*. *Astrophys. Space Sci.* 337, 107-113. doi 10.1007/s10509- 011-0821-8
[45] Zotos, E. E.,(2016(a)), *Fractal basins of attraction in the planar circular restricted three body problem with oblateness and radiation pressure*. *Astrophys. Space Sci.* 181(17). doi 10.1007/s10509-016-2769-1
[46] Zotos,E. E., (2016(b)), *Fractal basins boundaries and escape dynamics in a multi-well potential*. *Nonlinear Dynamics* 85, 1613- 1633. doi 10.1007/s11071-016-2782-5
[47] Zotos, E. E., (Oct 2016(c)), *Investigating the Newton-Raphson basins of attraction in the restricted three body problem with modified Newtonian gravity*. *J. Appl. Math. Comput.* 1-19. doi 10.1007/s12190-016-1061-4
[48] Zotos, E. E.,(2017), *Revealing the basins of convergence in the planar equilateral restricted four body problem*. *Astrophys. Space Sci.* 362(2). doi 10.1007/s10509-016-2973-z